Chapter 5

Reduced order modeling of 2D Burgers equation

Mehmet Önder Efe

Department of Electrical and Electronics Engineering, TOBB Economics and Technology University, Sögütözü, TR-06560 Ankara, Turkey

Modeling is a critically important stage in many engineering applications. Especially in control systems, a representative model constitutes the entity on which the design study is carried out. When the systems governed by partial differential equations (PDEs) are taken into consideration, it is seen that the traditional approaches of systems and control theory are not directly applicable. The PDE model undergoes an intermediate modeling procedure, that is, the dimension reduction. This fact is primarily because of the infinite dimensionality, in other words, the spatial continuity. The two-dimensional Burgers equation is considered as the example. Proper orthogonal decomposition (POD) is used for the order reduction and the chosen PDE is solved over a square domain, the corners of which for both state variables are the possible inputs for external stimuli. The results have shown that a useful low-dimensional model is achievable in standard state space, and the representational capability of the model is satisfactory.

5.1 Introduction

Developing low-dimensional models for partial differential equations (PDEs) is one of the active research topics today. Many physical phenomena are characterized by PDEs, and the understanding of them sometimes requires simple computational tools such as a reduced order model capturing the essential dynamics of the process. The two-dimensional (2D) Burgers equation is a good example to study the difficulties encountered in low-dimensional modeling of infinite dimensional systems. The reason is that the involved dynamics is governed by two coupled nonlinear PDEs introducing a significant amount of computational complexity. Referring to [1], the 2D Burgers equation is described by

$$w_t + \epsilon(w \cdot \nabla)w = \mu\nabla^2 w \tag{5.1}$$

SIVA: "CHAP05" — 2008/6/23 — 20:18 — PAGE 73 — #1

where $w(x, y, t) := (u(x, y, t)\ \ v(x, y, t))^T$, and $(x, y, t) \in [0, 1] \times [0, 1] \times [0, T]$, with T being some final time. 2D Burgers equation has been studied in the past for modeling traffic flows, shock waves and acoustic transmission. In [2–4], some variants of 2D Burgers equation have been considered with the goal of finding exact solutions under certain circumstances. Blender, on the other hand, postulates a method to obtain the solution of the PDE set in (5.1) iteratively [5]. Güngör [6] demonstrates that if suitable subalgebras can be defined, the PDE could be converted into an ordinary differential equation (ODE), but it is a major problem to find such subalgebras particularly for boundary control purposes. Nishinari *et al*. [7] focus on cellular automaton, which is extensively studied for developing models of traffic flow, fluids and immune systems, and therefore a good model to work on is a variant of Burgers equation. In [8], the dynamics that arises upon discretization of 2D Burgers equation is analyzed. The effects of chosen time step (Δt) for getting physically reasonable numerical solutions are elaborated. Wescott and Rizwan-uddin [9] present a computational technique to obtain the numerical solutions of PDEs having nonlinear convection terms like 2D Burgers equation and Navier–Stokes equations. The goal in [9] is to reduce the computation time without giving concessions from the accuracy. Boules and Eick [10] obtain the solution for a specific boundary regime and initial conditions. Using a truncated Fourier series expansion yields an autonomous ODE set, the solution of which approximates the numerical solution, and the derived model rebuilds the situation implied by the chosen initial and boundary conditions. Except [10], the works on 2D Burgers equation emphasize the similar difficulties as the motivating factors and focus on the solutions and solvability issues. This chapter, on the other hand, derives a nonautonomous ODE model that has external inputs explicitly and that is valid for some set of boundary conditions with zero initials.

When the one-dimensional (1D) version is taken into consideration, it is seen that the 1D Burgers equation has previously been considered for modeling and control system design purposes, and it has been shown in [11, 21] that the task is achievable, yet there are very few results reporting the modeling issues for vector PDE sets and higher dimensional cases as emphasized above. This chapter fills the gap between very simple models such as 1D heat flow or Burgers system and very complicated systems such as those reported in [22–24]. Clearly, the presented work is a step towards the goal of modeling and control of more complicated PDE systems.

This chapter approaches the modeling problem from a control specialist's point of view, that is, a suitable model reduction associated with a set of well-defined system inputs and a well-defined range of operating region. This process contains three major issues that need to be addressed appropriately. First issue is to collect the representative data and to exploit decomposition techniques for obtaining a set of ODEs. The next issue is to separate the effect of external stimuli from the other terms by utilizing the boundary conditions. The last issue is to validate the model. The considered process is continuous over a physical domain ($\Omega := [0, 1]\times[0,1]$), the boundaries of which are the possible entries of external stimuli for both $u(x, y, t)$ and $v(x, y, t)$. Choosing an adequately dense grid, say Ω_d, makes it possible to obtain a finite element representation of the process $w(x, y, t)$ over Ω_d. When the content of the observed data, say $w(x, y, t)$, is decomposed into spatial and temporal constituents ($u(x, y, t) \approx \sum_{i=1}^{R_L} \Phi_i(x, y)\alpha_i(t)$ and $v(x, y, t) \approx \sum_{i=1}^{R_L} \Psi_i(x, y)\alpha_i(t)$), the essence of spatial behavior appears as a set of spatial basis functions ($\Phi(x, y) = \{\Phi_1(x, y), \Phi_2(x, y), \ldots, \Phi_{R_L}(x, y)\}$ and $\Psi(x, y) = \{\Psi_1(x, y), \Psi_2(x, y), \ldots, \Psi_{R_L}(x, y)\}$, with R_L being a positive integer), and the essence of temporal evolution, $\alpha(t)$, appears as the solution of a set of ODEs obtained after utilizing the orthogonality properties of the spatial basis functions, that is, the eigenfunctions.

As suggested in the pioneering work of Lumley [25], the dimension reduction in systems having high orders can be done by utilizing proper orthogonal decomposition (POD), or

singular value decomposition (SVD) in cooperation with Galerkin projection [19, 22–24, 26–28], or balancing methods as discussed in the survey of Gügercin and Antoulas [29]. The decomposition-based methods exploit the sampled solutions (snapshots) obtained from the process and yield a set of temporal variables associated with a set of spatial basis functions [24, 26, 27, 30]. In order to obtain a useful approximation, the data, which is the raw information entering the modeling process, should contain coherent modes. The procedure, if it succeeds, yields a set of autonomous ODEs synthesizing the aforementioned temporal values. The reason that motivates us for using POD is twofold: First, it is based on the numerical data, and this fact makes it possible to derive a model where some instantaneous solutions of the process are measurable. Second, the POD is an efficient way to approximate the grammians of a given system [31], and this fact is critically important if the model is to be used for feedback system design.

Since the application of POD yields a set of autonomous ODEs, that is, no external inputs are present, the separation of boundary condition(s) (or the control input(s)) from the remaining terms becomes a key issue. For example, Krstić [18] describes a neatly selected Lyapunov function, and the expression in its time derivative enables us to apply integration by parts; then the boundary condition emerges in an explicit manner. Although the approach lets the designer manipulate Dirichlét and Neumann type boundary conditions on Burgers equation, it is still tedious to follow the same procedure for more complicated PDEs. This can be because of the high dimensionality of the PDE in particular, and difficulty in finding an appropriate Lyapunov function in general. Therefore, utilizing the numerical techniques is a practical alternative to describe reduced order models for complicated systems of PDEs. Obtaining the ODE model with explicitly stated external inputs is one important achievement of the overall modeling effort.

As pointed out in [20, 26], once the model is obtained, the final issue is to validate it. It has been shown in the mentioned references that the behavior of the resulting model is similar to the original system dynamics approximately over the frequency range covered in the model derivation phase. This restricts the operating conditions to particular frequencies, which is also addressed in this chapter.

The motivation of this chapter is to draw a clear path between a given PDE system and the representative finite dimensional nonautonomous ODE model. With this in mind, the chapter is organized as follows: Section 5.2 presents briefly the POD technique and its relevance to the modeling strategy. In Section 5.3, development of the reduced order ODE model for the 2D Burgers equation is postulated. The justification of the model, results and the contributions to the subject area are discussed in Section 5.4. Concluding remarks are given at the end of the chapter.

5.2 Proper orthogonal decomposition

Consider the ensemble $P_i \in \Re^{m\times n}$, $i = 1, 2, \ldots, N_s$, where N_s is the number of elements. Every element of this set corresponds to a snapshot observed from a process, say, for example, 2D Burgers equation given in (5.1) or

$$\begin{aligned} u_t &= \mu u_{xx} + \mu u_{yy} - \epsilon u u_x - \epsilon v u_y \\ v_t &= \mu v_{xx} + \mu v_{yy} - \epsilon u v_x - \epsilon v v_y, \end{aligned} \tag{5.2}$$

with ϵ and μ being known constants, and the subscripts x, y and t refer to the partial differentiation with respect to x, y and time, respectively. The continuous time process takes place over the

physical domain $\Omega := \{(x, y)|(x, y) \in [0, 1] \times [0, 1]\}$ and the solution is obtained on a grid denoted by Ω_{d}, which describes the coordinates of the pixels of every snapshot in the ensemble.

The goal is to find an orthonormal basis set letting us to write the solution as

$$\begin{pmatrix} u(x, y, t) \\ v(x, y, t) \end{pmatrix} \approx \begin{pmatrix} \hat{u}(x, y, t) \\ \hat{v}(x, y, t) \end{pmatrix} = \sum_{i=1}^{R_L} \alpha_i(t) \begin{pmatrix} \Phi_i(x, y) \\ \Psi_i(x, y) \end{pmatrix} \tag{5.3}$$

where $\alpha_i(t)$ is the temporal part, $\begin{pmatrix} \Phi_i(x, y) \\ \Psi_i(x, y) \end{pmatrix}$ is the spatial part, $\begin{pmatrix} \hat{u}(x, y, t) \\ \hat{v}(x, y, t) \end{pmatrix}$ is the finite element approximate of the infinite dimensional PDE and R_L is the number of independent basis functions that can be synthesized from the given ensemble, or equivalently the set of eigenfunctions that spans the space described by the ensemble. It will later be clear that the orthonormality of the elements of the basis set $\begin{pmatrix} \Phi_i(x, y) \\ \Psi_i(x, y) \end{pmatrix}$ for $i = 1, 2, \ldots, R_L$, and Galerkin projection technique let us obtain a finite dimensional set of dynamical equations. More explicitly, the inner product operator defined over the basis functions is described as

$$\left\langle \begin{pmatrix} \Phi_i \\ \Psi_i \end{pmatrix}, \begin{pmatrix} \Phi_j \\ \Psi_j \end{pmatrix} \right\rangle_{\Omega} := \iint_{\Omega} \left(\Phi_i \Phi_j + \Psi_i \Psi_j \right) \mathrm{d}\Omega = \delta_{ij} \tag{5.4}$$

where $\delta_{ij} = 1$ when $i = j$ and zero otherwise, that is, the Kronecker delta. With these definitions, the POD procedure can be summarized as follows:

Step 1. Define the concatenated process snapshot captured at time t as $P_t := \begin{pmatrix} U_t \\ V_t \end{pmatrix}$, where U_t and V_t are $R \times R$, P_t is $m \times n$ with $m = 2R$ and $n = R$, and R determines the spatial resolution. Without loss of generality, t could be an integer that is used to index the snapshots. Start calculating the $N_s \times N_s$ dimensional correlation matrix L, the (ij)-th entry of which is $L_{ij} := \langle P_i, P_j \rangle_{\Omega_{\mathrm{d}}}$, where $\langle ., . \rangle_{\Omega_{\mathrm{d}}}$ is the inner product operator defined over the chosen spatial grid Ω_{d}. Notice that the basis vectors $\begin{pmatrix} \Phi_i(x, y) \\ \Psi_i(x, y) \end{pmatrix}$ are defined over Ω, whereas the bases that are obtained numerically (the sampled forms) $\begin{pmatrix} \phi_i \\ \psi_i \end{pmatrix}$ are defined over Ω_{d} and, ϕ_i and ψ_i are $R \times R$ matrices. Therefore, we need the equivalent form of the used inner product, which is given as

$$\begin{aligned} \left\langle \begin{pmatrix} \phi_i \\ \psi_i \end{pmatrix}, \begin{pmatrix} \phi_j \\ \psi_j \end{pmatrix} \right\rangle_{\Omega_{\mathrm{d}}} &:= \frac{1}{N_s} \left(\phi_i \star \phi_j + \psi_i \star \psi_j \right) \\ &= \frac{1}{N_s} \sum_{p=1}^{R} \sum_{q=1}^{R} \phi_i(p, q)\phi_j(p, q) + \psi_i(p, q)\psi_j(p, q) \\ &= \delta_{ij}, \end{aligned} \tag{5.5}$$

where $\phi_a \star \phi_b := \sum_{i=1}^{R} \sum_{j=1}^{R} \phi_a(i, j)\phi_b(i, j)$, that is, $\star$ stands for the sum of all elements of a matrix that is obtained through elementwise multiplication of two matrices.

Step 2. Find the eigenvectors denoted by ξ_i and the associated eigenvalues (λ_i) of the symmetric matrix L. Sort them in a descending order in terms of the magnitudes of λ_i. Note that every ξ_i is an $N_s \times 1$ dimensional vector satisfying $\xi_i^T \xi_i = \frac{1}{\lambda_i}$; here, for simplicity of the exposition, we assume that the eigenvalues are distinct.

Step 3. Construct the basis set by utilizing the snapshots

$$\begin{pmatrix} \phi_i \\ \psi_i \end{pmatrix} = \sum_{k=1}^{N_s} \xi_{ik} P_k = \sum_{k=1}^{N_s} \begin{pmatrix} \xi_{ik} U_k \\ \xi_{ik} V_k \end{pmatrix}, \tag{5.6}$$

where ξ_{ik} is the k-th entry of the eigenvector ξ_i, and $i = 1, 2, ..., R_L$, where $R_L = \text{rank}(L)$. It can be shown that $\left\langle \begin{pmatrix} \phi_i \\ \psi_i \end{pmatrix}, \begin{pmatrix} \phi_j \\ \psi_j \end{pmatrix} \right\rangle_{\Omega_d} = \delta_{ij}$, with δ_{ij} being the Kronecker delta function. Notice that the basis functions are admixtures of the snapshots [21,24,26].

Step 4. Calculate the temporal coefficients. When $t = t_k$, taking the inner product of both sides of (5.3) with $\begin{pmatrix} \Phi_i \\ \Psi_i \end{pmatrix}$, the orthonormality property leads to

$$\alpha_i(t_k) = \left\langle \begin{pmatrix} \Phi_i(x, y) \\ \Psi_i(x, y) \end{pmatrix}, \begin{pmatrix} \hat{u}(x, y, t_k) \\ \hat{v}(x, y, t_k) \end{pmatrix} \right\rangle_{\Omega} = \left\langle \begin{pmatrix} \phi_i \\ \psi_i \end{pmatrix}, \begin{pmatrix} U_{t_k} \\ V_{t_k} \end{pmatrix} \right\rangle_{\Omega_d}, \tag{5.7}$$

Note that the temporal coefficients satisfy orthogonality properties over the discrete set $t_k \in \{t_1, t_2, \ldots, t_{N_s}\}$ (see Eq. (5.8)). For a more detailed discussion on the POD method, the reader is referred to [22–24, 26] and references therein,

$$\sum_{i=1}^{N_s} \left\langle \begin{pmatrix} U_i \\ V_i \end{pmatrix}, \begin{pmatrix} \phi_k \\ \psi_k \end{pmatrix} \right\rangle_{\Omega_d}^2 \approx \sum_{i=1}^{N_s} \alpha_k^2(t_i) = \lambda_k. \tag{5.8}$$

Underlying Assumption: The majority of works dealing with POD and model reduction applications presume that the flow is dominated by coherent modes and the quantities $\begin{pmatrix} u(x, y, t) \\ v(x, y, t) \end{pmatrix}$ and $\begin{pmatrix} \hat{u}(x, y, t) \\ \hat{v}(x, y, t) \end{pmatrix}$ are indistinguishable [19,22–24,26]. Because of the dominance of coherent modes, the typical spread of the eigenvalues of the correlation matrix L turns out to be logarithmic and the terms decay very rapidly in magnitude. This fact further enables to assume that a reduced order representation, say with M modes ($M \leq \min(R_L, N_s)$), can also be written as an equality

$$\begin{pmatrix} \hat{u}(x, y, t) \\ \hat{v}(x, y, t) \end{pmatrix} = \sum_{i=1}^{M} \alpha_i(t) \begin{pmatrix} \Phi_i(x, y) \\ \Psi_i(x, y) \end{pmatrix}, \tag{5.9}$$

and the reduced order model is derived under the assumption that (5.9) satisfies the governing PDE. Unsurprisingly, such an assumption results in a model having uncertainties; however, one should keep in mind that the goal is to find a model that matches the infinite dimensional system in some sense of approximation with typically $M \ll R_L \leq N_s$. To represent how good such an expansion is, a percent energy measure is defined as follows:

$$E = \frac{\sum_{i=1}^{M} \lambda_i}{\sum_{i=1}^{R_L} \lambda_i} \times 100\%, \tag{5.10}$$

where the tendency of $E \to 100\%$ means that the model captures the dynamical information contained in the snapshots well. Conversely, an insufficient model will be obtained if E is far below 100%. The second part of the underlying assumption emphasizes the compliance between the numerical solution obtained over a finite-dimensional grid defined over Ω_d and the true solution

defined over Ω. This statement makes it possible to use a snapshot as an entity representing the true dynamics at a particular instant of time.

In Section 5.3, we demonstrate how the boundary condition is transformed to an explicit control input in the ODEs.

5.3 Development of the ODE model

According to the underlying assumption of POD-based model reduction scheme, the approximate solution in Eq. (5.9) must satisfy the PDE in Eq. (5.2). Substituting Eq. (5.9) into Eq. (5.2) and taking the inner product of both sides with $\begin{pmatrix} \Phi_k \\ \Psi_k \end{pmatrix}$ yields

$$\dot{\alpha}_k = \mu \sum_{i=1}^{M} \alpha_i \left\langle \begin{pmatrix} \Phi_{xxi} + \Phi_{yyi} \\ \Psi_{xxi} + \Psi_{yyi} \end{pmatrix}, \begin{pmatrix} \Phi_k \\ \Psi_k \end{pmatrix} \right\rangle_{\Omega} - \epsilon \sum_{i=1}^{M} \sum_{j=1}^{M} \alpha_i \alpha_j \left\langle \begin{pmatrix} \Phi_i \Phi_{xj} + \Psi_i \Phi_{yj} \\ \Phi_i \Psi_{xj} + \Psi_i \Psi_{yj} \end{pmatrix}, \begin{pmatrix} \Phi_k \\ \Psi_k \end{pmatrix} \right\rangle_{\Omega}. \tag{5.11}$$

Notice that the orthonormality property of the basis vectors leaves the $\dot{\alpha}_k$ term alone on the left-hand side. Equivalently, by using the numerical quantities, the expression above can be rewritten as follows:

$$\begin{aligned} \dot{\alpha}_k = {} & \mu \sum_{i=1}^{M} \alpha_i \left\langle \begin{pmatrix} \phi_{xxi} + \phi_{yyi} \\ \psi_{xxi} + \psi_{yyi} \end{pmatrix}, \begin{pmatrix} \phi_k \\ \psi_k \end{pmatrix} \right\rangle_{\Omega_{\mathrm{d}}} \\ & - \epsilon \sum_{i=1}^{M} \sum_{j=1}^{M} \alpha_i \alpha_j \left\langle \begin{pmatrix} \phi_i \circ \phi_{xj} + \psi_i \circ \phi_{yj} \\ \phi_i \circ \psi_{xj} + \psi_i \circ \psi_{yj} \end{pmatrix}, \begin{pmatrix} \phi_k \\ \psi_k \end{pmatrix} \right\rangle_{\Omega_{\mathrm{d}}}, \end{aligned} \tag{5.12}$$

where $\circ$ stands for the elementwise multiplication of two matrices.

Although it is straightforward to conclude with the ODEs given in Eqs. (5.11) and (5.12), it is apparent that these equations do not have the boundary conditions (external inputs) explicitly. Chosen initial conditions and boundary excitation regime determine the solution, and the ODEs above resynthesize the temporal variables, $\alpha_i(t)$, associated with that particular solution (see Eq. (5.9)). It is clear that such an ODE model is useless as it is specific to the chosen boundary conditions. Our goal is to obtain a model that has external inputs explicitly and that can be used for the boundary conditions other than the used ones. For this purpose, a method needs to be postulated for separating the boundary excitations appropriately. According to the definition of the inner product operator, it should be obvious that

$$\left\langle \begin{pmatrix} \phi_i \\ \psi_i \end{pmatrix}, \begin{pmatrix} \phi_j \\ \psi_j \end{pmatrix} \right\rangle_{\Omega_{\mathrm{d}}} = \left\langle \begin{pmatrix} \phi_i \\ \psi_i \end{pmatrix}, \begin{pmatrix} \phi_j \\ \psi_j \end{pmatrix} \right\rangle_{\Omega_{\mathrm{d}} \setminus \partial\Omega_{\mathrm{d}}} + \left\langle \begin{pmatrix} \phi_i \\ \psi_i \end{pmatrix}, \begin{pmatrix} \phi_j \\ \psi_j \end{pmatrix} \right\rangle_{\partial\Omega_{\mathrm{d}}}. \tag{5.13}$$

In Eq. (5.13), $\partial\Omega_{\mathrm{d}}$ indicates the boundaries of the considered domain where the boundary conditions are specified freely. In this chapter, we study pointwise boundary excitations; alternatively, one could prescribe the boundary conditions along some subdomain of $\partial\Omega_{\mathrm{d}}$. The approach presented in this chapter can be extended to handle such cases.

Denote (x_c, y_c) as one of the points at which the solution is independently specified (i.e., the boundary) and (p_{x_c}, q_{y_c}) as the row and column numbers of this location in matrices ϕ_i and ψ_i.

Note that the prescribed solution in Eq. (5.9) must be satisfied also at (x_c, y_c), i.e., we have

$$\hat{u}(x_c, y_c, t) := \gamma_{x_c y_c u}(t) = \sum_{i=1}^{M} \alpha_i(t)\phi_i(p_{x_c}, q_{y_c}) \tag{5.14a}$$

$$\hat{v}(x_c, y_c, t) := \gamma_{x_c y_c v}(t) = \sum_{i=1}^{M} \alpha_i(t)\psi_i(p_{x_c}, q_{y_c}) \tag{5.14b}$$

or, equivalently, we can rewrite these equations as

$$\alpha_k(t)\phi_k(p_{x_c}, q_{y_c}) = \gamma_{x_c y_c u}(t) - \sum_{i=1}^{M} (1 - \delta_{ik})\, \alpha_i(t)\phi_i(p_{x_c}, q_{y_c}), \tag{5.15}$$

$$\alpha_k(t)\psi_k(p_{x_c}, q_{y_c}) = \gamma_{x_c y_c v}(t) - \sum_{i=1}^{M} (1 - \delta_{ik})\, \alpha_i(t)\psi_i(p_{x_c}, q_{y_c}). \tag{5.16}$$

Since we consider the problem on a square domain, Ω_{d}, for both states, every corner can be a possible entry for the external excitations and we may have at most eight distinct inputs for this system. Once the Dirichlét type corner conditions are specified, the numerical solutions $u(x, y, t)$ and $v(x, y, t)$ on $x = 0$, $y = 0$, $x = 1$ and $y = 1$ segments of Ω_{d} need to be obtained. This can be achieved by setting the relevant partial derivatives in Eq. (5.2) to zero and by solving the resulting PDE. For example, we solve

$$\begin{aligned} u_t &= \mu u_{yy} - \epsilon v u_y \\ v_t &= \mu v_{yy} - \epsilon v v_y \end{aligned} \tag{5.17}$$

along $x = 1$ segment, which is a significant subtlety of moving from 1D to 2D. For the simplicity of the exposition, assume $x_c = 0$ and $y_c = 0$ ($(p_{x_c}, q_{y_c}) = (1, 1)$) is the chosen corner, and rewrite Eq. (5.12) as follows:

$$\begin{aligned} \dot{\alpha}_k = {} & \frac{\mu}{N_s} \sum_{i=1}^{M} \alpha_i \left(\left(\phi_{xxi} + \phi_{yyi}\right) \star \phi_k + \left(\psi_{xxi} + \psi_{yyi}\right) \star \psi_k \right) \\ & - \frac{\epsilon}{N_s} \sum_{i=1}^{M} \sum_{j=1}^{M} \alpha_i \alpha_j \left(\left(\phi_i \circ \phi_{xj} + \psi_i \circ \phi_{yj}\right) \star \phi_k \right) + \left(\left(\phi_i \circ \psi_{xj} + \psi_i \circ \psi_{yj}\right) \star \psi_k \right). \end{aligned} \tag{5.18}$$

Let $\zeta_i := \phi_{xxi} + \phi_{yyi}$ and $\theta_i := \psi_{xxi} + \psi_{yyi}$, and rearrange Eq. (5.18) as given below

$$\begin{aligned} \dot{\alpha}_k = {} & \frac{\mu}{N_s} \sum_{i=1}^{M} \alpha_i \left(\zeta_i \star \phi_k + \theta_i \star \psi_k \right) \\ & - \frac{\epsilon}{N_s} \sum_{i=1}^{M} \sum_{j=1}^{M} \alpha_i \alpha_j \left(\left(\phi_i \circ \phi_{xj} + \psi_i \circ \phi_{yj}\right) \star \phi_k \right) + \left(\left(\phi_i \circ \psi_{xj} + \psi_i \circ \psi_{yj}\right) \star \psi_k \right). \end{aligned} \tag{5.19}$$

Define $\phi'_k = \{\phi'_k | \phi'_k(i, j) = \phi_k(i, j) \text{ when } i \neq p_{x_c}, j \neq q_{y_c}, \text{ and } \phi'_k(p_{x_c}, q_{y_c}) = 0\}$ and $\zeta'_k = \{\zeta'_k | \zeta'_k(i, j) = \zeta_k(i, j) \text{ when } i \neq p_{x_c}, j \neq q_{y_c}, \text{ and } \zeta'_k(p_{x_c}, q_{y_c}) = 0\}$ and so on. By

this means, the matrices used in the derivation have zero values corresponding to the external excitation entries. Now we can explicitly write the first term in Eq. (5.19) as follows:

$$\begin{aligned}\sum_{i=1}^{M}\alpha_i\zeta_i\star\phi_k &= \sum_{i=1}^{M}\alpha_i\left(\zeta_i'\star\phi_k' + \zeta_i(1,1)\phi_k(1,1)\right)\\ &= \sum_{i=1}^{M}\alpha_i\left(\zeta_i'\star\phi_k'\right) + \sum_{i=1}^{M}\alpha_i\zeta_i(1,1)\phi_k(1,1)\\ &= \sum_{i=1}^{M}\alpha_i\left(\zeta_i'\star\phi_k'\right) + \left(\alpha_k\zeta_k(1,1)\phi_k(1,1) + \sum_{i=1}^{M}(1-\delta_{ik})\alpha_i\zeta_i(1,1)\phi_k(1,1)\right).\end{aligned} \tag{5.20}$$

Utilizing Eq. (5.15) for the term $\alpha_k\zeta_k(1,1)\phi_k(1,1)$, we get

$$\alpha_k\zeta_k(1,1)\phi_k(1,1) = \gamma_{00u}(t)\zeta_k(1,1) - \sum_{i=1}^{M}(1-\delta_{ik})\alpha_i\zeta_k(1,1)\phi_i(1,1). \tag{5.21}$$

Inserting Eq. (5.21) into Eq. (5.20) yields the following:

$$\begin{aligned}\sum_{i=1}^{M}\alpha_i\zeta_i\star\phi_k &= \gamma_{00u}(t)\zeta_k(1,1) + \sum_{i=1}^{M}\alpha_i\left(\zeta_i'\star\phi_k'\right)\\ &\quad + \sum_{i=1}^{M}(1-\delta_{ik})\alpha_i\left(\zeta_i(1,1)\phi_k(1,1) - \zeta_k(1,1)\phi_i(1,1)\right)\\ &= \gamma_{00u}(t)\zeta_k(1,1) + \sum_{i=1}^{M}\alpha_i\left(\zeta_i'\star\phi_k'\right)\\ &\quad + \sum_{i=1}^{M}\alpha_i\left(\zeta_i(1,1)\phi_k(1,1) - \zeta_k(1,1)\phi_i(1,1)\right)\\ &= \gamma_{00u}(t)\zeta_k(1,1) + \sum_{i=1}^{M}\alpha_i\left(\zeta_i'\star\phi_k'\right)\\ &\quad + \sum_{i=1}^{M}\alpha_i\left(\zeta_i(1,1)\phi_k(1,1) - \zeta_k(1,1)\phi_i(1,1)\right)\\ &= \gamma_{00u}(t)\zeta_k(1,1) + \sum_{i=1}^{M}\alpha_i\left(\zeta_i\star\phi_k - \zeta_k(1,1)\phi_i(1,1)\right).\end{aligned} \tag{5.22}$$

For the second term in the first summation of Eq. (5.19), this result implies the equality in Eq. (5.23), and the concatenated form is given in Eq. (5.24),

$$\sum_{i=1}^{M}\alpha_i(\theta_i\star\psi_k) = \gamma_{00v}(t)\theta_k(1,1) + \sum_{i=1}^{M}\alpha_i\left(\theta_i\star\psi_k - \theta_k(1,1)\psi_i(1,1)\right). \tag{5.23}$$

$$\sum_{i=1}^{M} \alpha_i \left(\zeta_i \star \phi_k + \theta_i \star \psi_k\right) = \gamma_{00u}(t)\zeta_k(1,1) + \gamma_{00v}(t)\theta_k(1,1)$$
$$+ \sum_{i=1}^{M} \alpha_i \left(\zeta_i \star \phi_k + \theta_i \star \psi_k - \zeta_k(1,1)\phi_i(1,1) - \theta_k(1,1)\psi_i(1,1)\right). \tag{5.24}$$

In the rest of this section, we will apply the same reasoning to the terms seen in the second line of Eq. (5.19). For this purpose, consider the first term,

$$\sum_{i=1}^{M}\sum_{j=1}^{M} \alpha_i\alpha_j \left(\left(\phi_i \circ \phi_{xj}\right) \star \phi_k\right) = \sum_{i=1}^{M}\sum_{j=1}^{M} \alpha_i\alpha_j \left(\left(\phi_i' \circ \phi_{xj}'\right) \star \phi_k' + \phi_i(1,1)\phi_{xj}(1,1)\phi_k(1,1)\right), \tag{5.25}$$

where we have

$$\sum_{i=1}^{M}\sum_{j=1}^{M} \alpha_i\alpha_j\phi_i(1,1)\phi_{xj}(1,1)\phi_k(1,1) = \phi_k(1,1)\sum_{i=1}^{M} \alpha_i\phi_i(1,1)\sum_{j=1}^{M} \alpha_j\phi_{xj}(1,1)$$
$$= \phi_k(1,1)\gamma_{00u}\sum_{j=1}^{M} \alpha_j\phi_{xj}(1,1). \tag{5.26}$$

Inserting Eq. (5.26) into Eq. (5.25) results in Eq. (5.27), and applying the same reasoning for the remaining three terms of Eq. (5.19) gives the equalities in Eqs. (5.28)–(5.30):

$$\sum_{i=1}^{M}\sum_{j=1}^{M} \alpha_i\alpha_j \left(\left(\phi_i \circ \phi_{xj}\right) \star \phi_k\right) = \sum_{i=1}^{M}\sum_{j=1}^{M} \alpha_i\alpha_j \left(\left(\phi_i' \circ \phi_{xj}'\right) \star \phi_k'\right)$$
$$+ \gamma_{00u}\sum_{j=1}^{M} \alpha_j\phi_k(1,1)\phi_{xj}(1,1), \tag{5.27}$$
$$\sum_{i=1}^{M}\sum_{j=1}^{M} \alpha_i\alpha_j \left(\left(\psi_i \circ \phi_{yj}\right) \star \phi_k\right) = \sum_{i=1}^{M}\sum_{j=1}^{M} \alpha_i\alpha_j \left(\left(\psi_i' \circ \phi_{yj}'\right) \star \phi_k'\right)$$
$$+ \gamma_{00v}\sum_{j=1}^{M} \alpha_j\phi_k(1,1)\phi_{yj}(1,1), \tag{5.28}$$
$$\sum_{i=1}^{M}\sum_{j=1}^{M} \alpha_i\alpha_j \left(\left(\phi_i \circ \psi_{xj}\right) \star \psi_k\right) = \sum_{i=1}^{M}\sum_{j=1}^{M} \alpha_i\alpha_j \left(\left(\phi_i' \circ \psi_{xj}'\right) \star \psi_k'\right)$$
$$+ \gamma_{00u}\sum_{j=1}^{M} \alpha_j\psi_k(1,1)\psi_{xj}(1,1), \tag{5.29}$$

$$\sum_{i=1}^{M}\sum_{j=1}^{M}\alpha_i\alpha_j\left(\left(\psi_i\circ\psi_{yj}\right)\star\psi_k\right)=\sum_{i=1}^{M}\sum_{j=1}^{M}\alpha_i\alpha_j\left(\left(\psi_i'\circ\psi_{yj}'\right)\star\psi_k'\right)$$
$$+\gamma_{00v}\sum_{j=1}^{M}\alpha_j\psi_k(1,1)\psi_{yj}(1,1). \tag{5.30}$$

According to the above derivation, the low-dimensional model for the 2D Burgers equation can be given by

$$\dot{\mathcal{X}}(t)=\mathcal{A}\mathcal{X}(t)-\mathcal{B}\left(\mathcal{X}(t)\right)+\mathcal{C}\Gamma(t)-\mathcal{D}(\mathcal{X}(t),\Gamma(t)), \tag{5.31}$$

where $\mathcal{X}(t)=\left(\alpha_1(t)\,\alpha_2(t)\cdots\alpha_M(t)\right)^T$, $\Gamma(t)=\left(\gamma_{00u}(t)\,\gamma_{00v}(t)\right)^T$, $\mathcal{A}$ is $M\times M$, $\mathcal{B}$ is $M\times 1$, $\mathcal{C}$ is $M\times 2$ and $\mathcal{D}$ is $M\times 1$. From Eq. (5.24), we can write the (ki)-th entry of matrix $\mathcal{A}$ and k-th row of matrix $\mathcal{C}$ as follows:

$$(\mathcal{A})_{ki}=\frac{\mu}{N_s}\left(\zeta_i\star\phi_k+\theta_i\star\psi_k-\zeta_k(1,1)\phi_i(1,1)-\theta_k(1,1)\psi_i(1,1)\right), \tag{5.32}$$

$$(\mathcal{C})_k=\frac{\mu}{N_s}\left(\zeta_k(1,1)\;\;\theta_k(1,1)\right). \tag{5.33}$$

where $k, i=1,2,\ldots,M$. Similarly, from Eqs. (5.27)–(5.30), it is seen that

$$\mathcal{B}(\mathcal{X})=\left(\mathcal{X}^T B_1\mathcal{X}\mathcal{X}^T B_2\mathcal{X}\cdots\mathcal{X}^{\mathrm{T}}B_M\mathcal{X}\right)^T \tag{5.34}$$

where the ij-th entry of matrix B_k is

$$(B_k)_{ij}=\frac{\epsilon}{N_s}\left(\left(\phi_i'\circ\phi_{xj}'\right)\star\phi_k'+\left(\psi_i'\circ\phi_{yj}'\right)\star\phi_k'+\left(\phi_i'\circ\psi_{xj}'\right)\star\psi_k'+\left(\psi_i'\circ\psi_{yj}'\right)\star\psi_k'\right), \tag{5.35}$$

and the k-th row entry of vector $\mathcal{D}$ is computed as

$$(\mathcal{D})_k=\gamma_{00u}\frac{\epsilon}{N_s}\sum_{j=1}^{M}\alpha_j\left(\phi_k(1,1)\phi_{xj}(1,1)+\psi_k(1,1)\psi_{xj}(1,1)\right)$$
$$+\gamma_{00v}\frac{\epsilon}{N_s}\sum_{j=1}^{M}\alpha_j\left(\phi_k(1,1)\phi_{yj}(1,1)+\psi_k(1,1)\psi_{yj}(1,1)\right) \tag{5.36}$$

or

$$\mathcal{D}=D_u\mathcal{X}\gamma_{00u}+D_v\mathcal{X}\gamma_{00v} \tag{5.37}$$

where D_u and D_v are $M\times M$ matrices and the (kj)-th entry is computed as

$$(D_u)_{kj}=\frac{\epsilon}{N_s}\left(\phi_k(1,1)\phi_{xj}(1,1)+\psi_k(1,1)\psi_{xj}(1,1)\right), \tag{5.38}$$

and

$$(D_v)_{kj}=\frac{\epsilon}{N_s}\left(\phi_k(1,1)\phi_{yj}(1,1)+\psi_k(1,1)\psi_{yj}(1,1)\right), \tag{5.39}$$

with $k, j=1,2,\ldots,M$. According to the derivation discussed in this section, once the initial and boundary conditions are specified, one can get a dynamic model that captures the essential features

of the solution. Although we have derived the model by assuming the external excitation enters at a single point for u and v dynamics, it is straightforward to apply the scheme for obtaining a model having up to eight inputs. In Section 5.4, the model is validated through some examples.

5.4 Justification of the model

In order to obtain the model, the 2D Burgers equation in Eq. (5.1) is solved for the boundary conditions given as

$$\begin{aligned} \gamma_{00u}(t) &= \sin(1000\pi t(T-t)) \\ \gamma_{00v}(t) &= \cos\left(1000\pi t\left(\frac{T}{2}-t\right)\right). \end{aligned} \tag{5.40}$$

The time plots and the fast Fourier transforms (FFT) of the signals above are depicted in Fig. 5.1. The reason that drives us to choose such signals is the spectral richness. If the spectral content of the excitations are rich enough, the resulting model is more likely to operate properly over the covered frequency range [20, 21]. The other important parameters of the simulation are tabulated in Table 5.1. The numerical solution is obtained through Crank–Nicholson method with zero initial conditions [32], and after the application of the modeling procedure discussed in Section 5.3, a model is obtained in the form of Eq. (5.31).

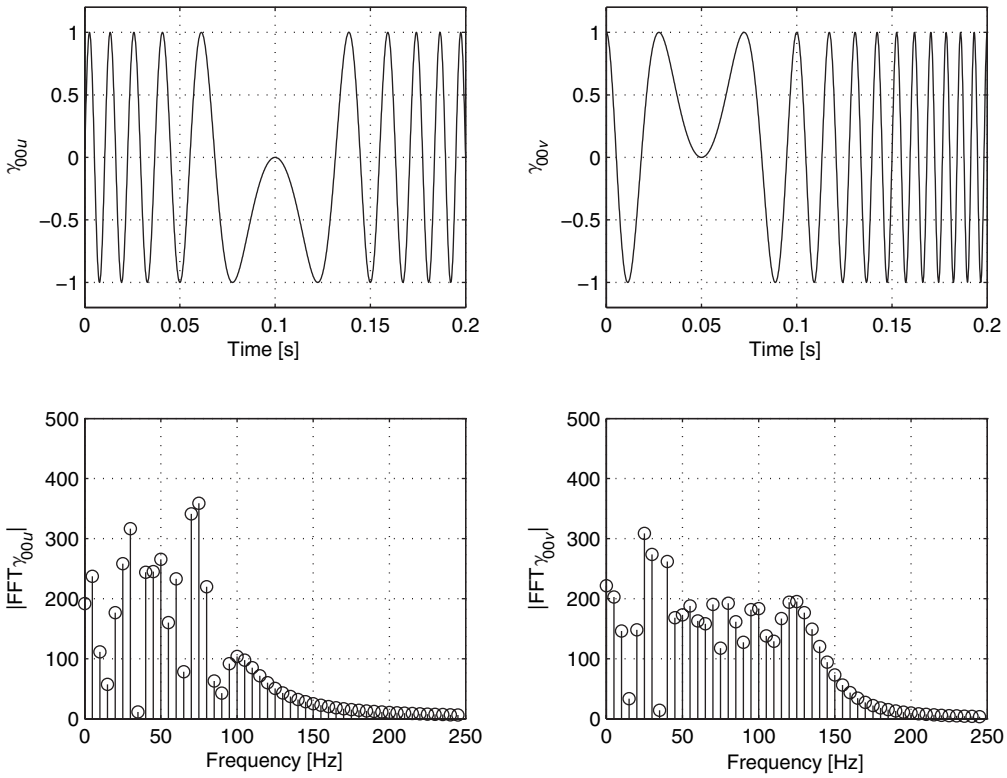

Figure 5.1: Boundary signals used for model derivation

Table 5.1: Simulation settings

R	25
M	8
Δt	0.1 ms
T	0.2 s
N_s	201
ϵ	1
μ	5

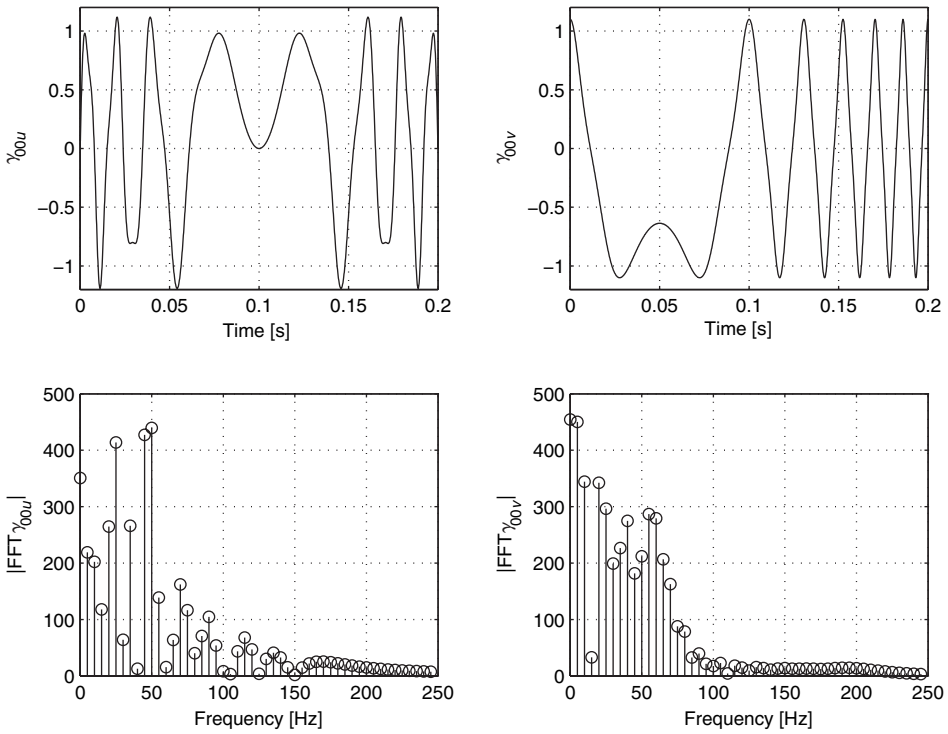

Figure 5.2: First set of boundary signals that are used for model validation

It has been observed that the eigenvalues (λ_i) decay very rapidly, and the captured energy content described by Eq. (5.10) is 99.9021%, which is found acceptable. The justification has been done with the same settings as shown in Table 5.1, and the first set of boundary excitations that are used in the model validation phase are

$$\begin{aligned}\gamma_{00u}(t) &= \sin(700\pi t(T-t)) + 0.2\sin(1700\pi t(T-t)),\\ \gamma_{00v}(t) &= \cos\left(500\pi t\left(\frac{T}{2}-t\right)\right) + 0.1\cos\left(1500\pi t\left(\frac{T}{2}-t\right)\right).\end{aligned} \tag{5.41}$$

Figure 5.2 illustrates these signals and the low frequency appearance of their FFT magnitude plots. The PDE is solved for this new case and the $\alpha_i(t)$ values are obtained by using Eq. (5.7), which yields the desired values. On the other hand, the model had already been developed, and it is simulated for the test boundary conditions in Eq. (5.41) with zero initials. The outcome is

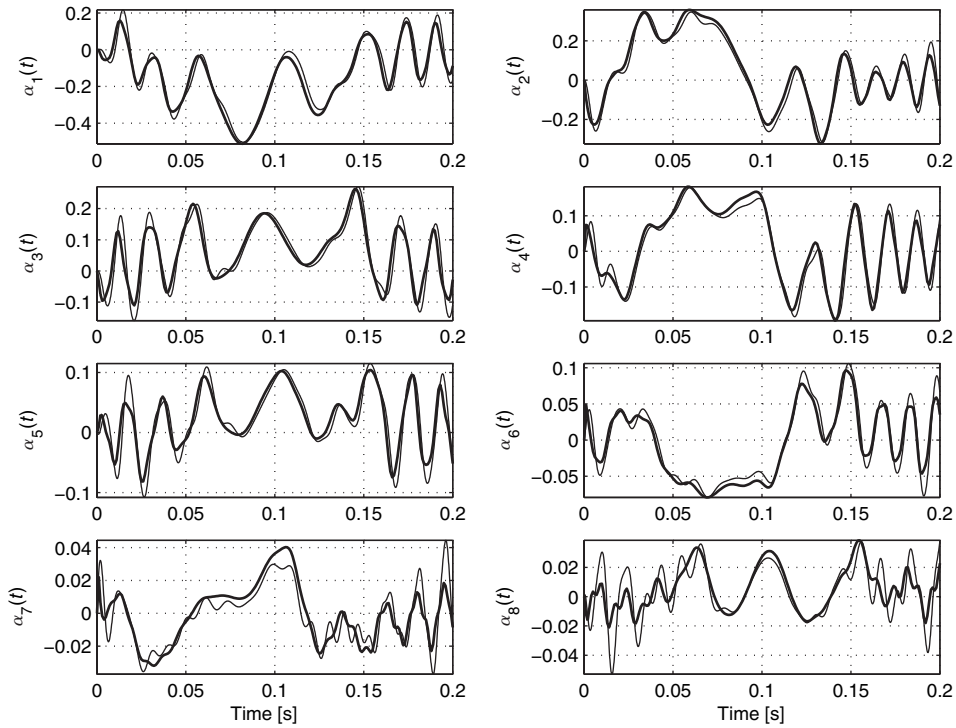

Figure 5.3: The desired values (thick curves) of $\alpha_i(t)$ and the obtained values (thin curves) for the first set of test conditions

expected to approximate the desired ones if the algorithm succeeds. The results are shown in Fig. 5.3, where the first remark is the number of ODEs that provided this result. With $M = 8$ modes (ODEs), the task can be achieved to the extent seen in Fig. 5.3. For the first five modes, the match is quite good, yet as the mode number increases the dissimilarity between the desired and generated values become more distinguishable. Since the dominance of the corresponding modes decrease logarithmically, as seen from Fig. 5.3 as well, so do their effect on the overall result. Therefore, the similarity of the first few modes is more substantial than the similarity of modes having high index numbers. A rough look at the eight subplots of Fig. 5.3 altogether gives the idea of a successful approximation from a higher dimensionality to low orders, which is the goal of this chapter.

We have repeated our tests for an extensive set of test signals. The correlation between the model performance and spectral content of the external excitations is seen empirically. To clarify this further, consider the second set of boundary conditions described by Eq. (5.42), which are depicted in Fig. 5.4.

$$\begin{aligned}\gamma_{00u}(t) &= \sin\left(700\pi t\left(\frac{T}{7}-t\right)\right)+0.2\sin\left(1700\pi t\left(\frac{T}{4}-t\right)\right),\\ \gamma_{00v}(t) &= \sin(2000\pi t(T-t)).\end{aligned} \tag{5.42}$$

A comparison of the Figs. 5.2 and 5.4, and Figs. 5.3 and 5.5 stipulate that the second set of boundary conditions displays sharper fluctuations than the first set, and therefore they spread over

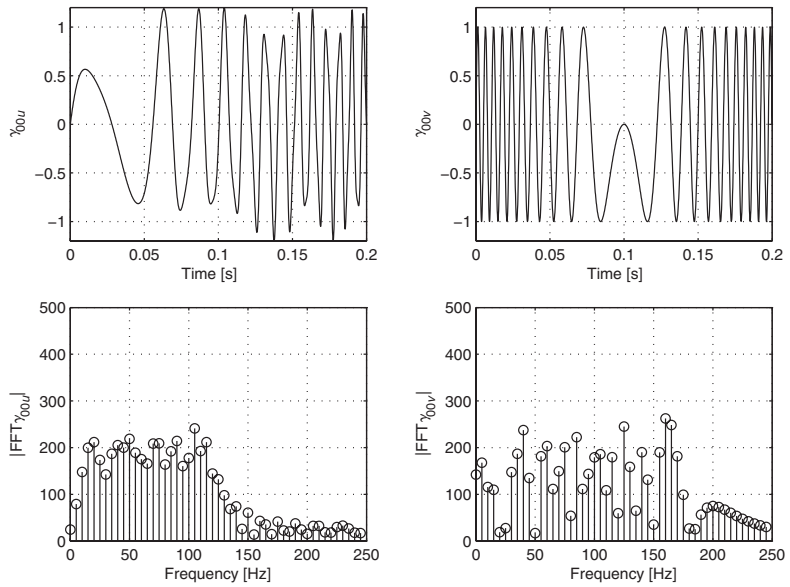

Figure 5.4: Second set of boundary signals that are used for model validation

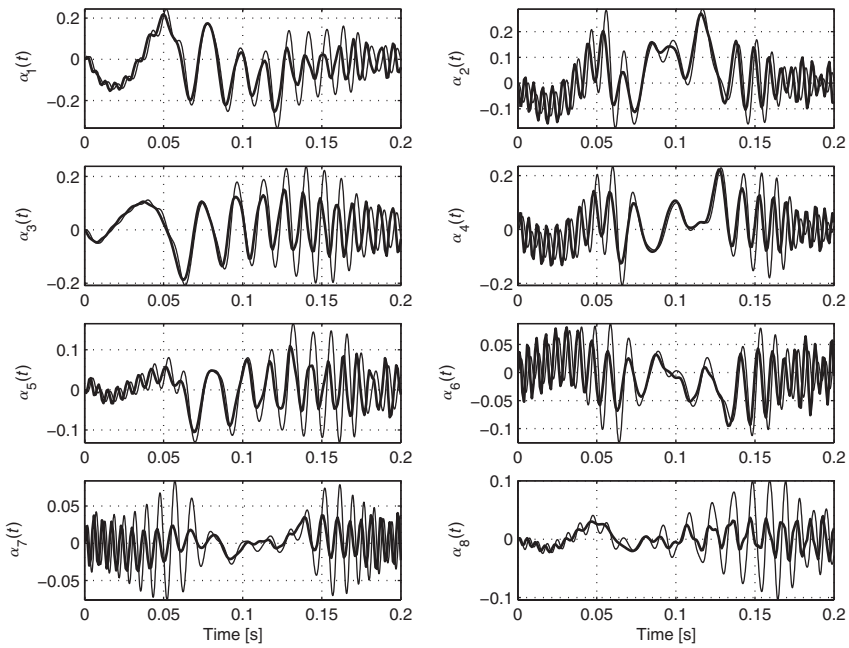

Figure 5.5: The desired values (thick curves) of $\alpha_i(t)$ and the obtained values (thin curves) for the second set of test conditions

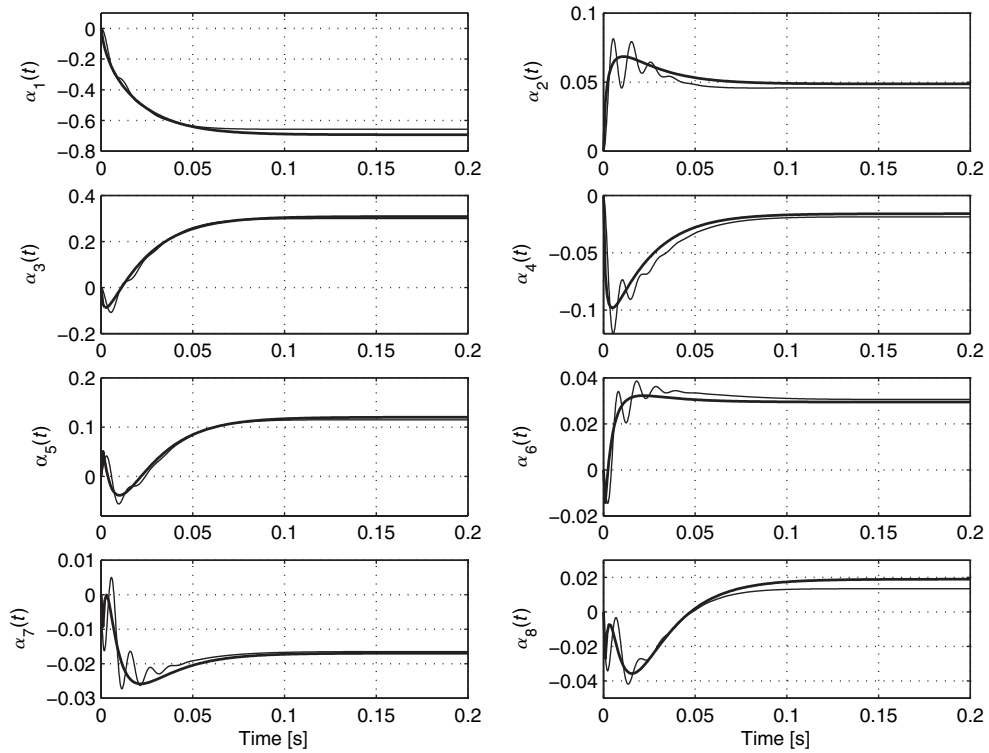

Figure 5.6: The desired values (thick curves) of $\alpha_i(t)$ and the obtained values (thin curves) for constant boundary conditions

a wider range in the frequency spectrum (see Fig. 5.4, bottom row). Qualitatively, the second set of boundary signals are dissimilar from the first set in the sense of spectral compositions. According to this, the results depicted in Figs. 5.3 and 5.5 support the following claim: The descriptive nature of the signals used in the model derivation is inherited by the developed dynamical model, and the signals that do not resemble to the model derivation conditions make the system fail, depending on the level of dissimilarity between the model derivation and validation signals. The dependence on the spectral content is an important conclusion determining the features and limitations of the low order model. Although it is very clear in Fig. 5.5 that the smooth parts of the temporal variables are reconstructed well, the performance where the signals change quickly is low. The same conclusion is visible also on the results seen in Fig. 5.3.

Another issue is to figure out the very low frequency behavior. For this purpose we have chosen constant boundary conditions, and set $\gamma_{00u}(t) = 1$ and $\gamma_{00v}(t) = -0.8$. The obtained results are illustrated in Fig. 5.6. The idea that we infer from the behavior of temporal variables shown in Figs. 5.3, 5.5 and 5.6 claim that the dynamic model is valid on a frequency region that is from zero to some upper value determined by the model derivation conditions. According to the results of this study, it is fair to claim that the dynamic model in Eq. (5.31) functions properly upto 100 Hz. Considering the results obtained in [10], it is seen that the presented work achieves the modeling goal with a few ODEs and associated spatial eigenfunctions.

A natural issue that needs to be highlighted is the way of improving obtained results. Expectedly, increasing the grid fineness, decreasing Δt, increasing the number of snapshots entering the POD procedure (N_s) and increasing the number of modes (M) are the alternatives that result in

better model performance, yet the price paid for this improvement is the increased computational intensity.

5.5 Conclusions

The research on flow modeling is drawing an ever-increasing attention [33–36]. One of the central issues in this field is the order reduction of the infinite dimensional model. Toward this goal, POD is one alternative among many others (see e.g. [29,33–36] and references therein). Its capability of capturing the essential dynamics dominating the entire physical phenomena makes POD preferable in the research on flow systems.

This chapter focuses on the low-dimensional modeling of 2D Burgers equation. The driving facts for focusing on this system are its nonlinear, coupled and vector-valued PDE nature. Once the POD algorithm is implemented, it is seen that the resulting ODE model is an autonomous one, and a method to overcome this problem needs to be developed. One major contribution of this chapter is on this issue, that is, the separation of boundary terms to obtain a nonautonomous ODE model is demonstrated step by step on such a complicated system. The second contribution of this chapter is its emphasis on the locality of the developed low order models. This feature is illustrated with an example. It is seen that the conditions used in the model derivation are critically important and the POD procedure has a natural propensity to build models that are valid on particular conditions. With these results, the present work advances the subject area to the establishment of a clear connection between state space methods of control theory and complex infinite dimensional systems of PDEs. The fact that this connection is built through the numerical observations from the infinite dimensional process is worthwhile to stress the applicability of the discussed modeling effort for other systems of PDEs. The simplicity of the final model is another merit of the presented approach.

Acknowledgments

The author would like to thank Prof. H. Özbay, Prof. M. Samimy, Dr. J. H. Myatt, Dr. J. DeBonis, Dr. R. C. Camphouse, Dr. P. Yan, X. Yuan and E. Caraballo for fruitful discussions in devising the presented work.

References

[1] J. Donea and A. Huerta. *Finite Element Methods for Flow Problems*. West Sussex: John Wiley & Sons, pp. 252–253, 2003.

[2] Sirendaoreji. Exact solutions of the two-dimensional Burgers equation. *Journal of Physics A: Mathematical and General*, 32:6897–6900, 1999.

[3] L. Hietarinta. Comments on Exact solutions of the teo-dimensional Burgers equation. *Journal of Physics A: Mathematical and General*, 33:5157–5158, 2000.

[4] Z. Zhu. Exact solutions for a two-dimensional KdV-Burgers-type equation. *Chinese Journal of Physics*, 34(4):1101–1105, 1996.

[5] R. Blender. Iterative solution of nonlinear partial-differential equations. *Journal of Physics A: Mathematical and General*, 24(10):L509–L512, 1991.

[6] F. Güngör. Symmetries and invariant solutions of the two-dimensional variable coefficient Burgers equation. *Journal of Physics A: Mathematical and General*, 34:4313–4321, 2001.

[7] K. Nishinari, J. Matsukidaira and D. Takahashi. Two-dimensional Burgers cellular automaton. *Journal of the Physical Society of Japan*, 70(8):2267–2272, 2001.

[8] I. Hataue. Mathematical and numerical analyses of dynamical structure of numerical solutions of two-dimensional fluid equations. *Journal of the Physical Society of Japan*, 67(6): 1895–1911, 1998.

[9] B. L. Wescott and Rizwan-uddin. An efficient formulation of the modified nodal integral method and application to the two-dimensional Burgers equation. *Nuclear Science and Engineering*, 139(3):293–305, 2001.

[10] A. N. Boules and I. J. Eick. A spectral approximation of the two-dimensional Burgers equation. *Indian Journal of Pure and Applied Mathematics*, 34(2):299–309, 2003.

[11] M. Hinze and S. Volkwein. Analysis of instantaneous control for Burgers equation. *Nonlinear Analysis*, 50:1–26, 2002.

[12] J. A. Burns, B. B. King and L. Zietsman. On the computation of singular functional gains for linear quadratic optimal boundary control problems. *Proceedings of the 3rd Theoretical Fluid Mechanics Meeting*, St. Louis, USA, 24–26 June, AIAA 2002-3074, 2002.

[13] J. A. Burns, B. B. King, A. D. Rubio and L. Zietsman. Functional gain computations for feedback control of a thermal fluid. *Proceedings of the 3rd Theoretical Fluid Mechanics Meeting*, St. Louis, USA, 24–26 June, AIAA 2002-2992, 2002.

[14] R. Vedantham. Optimal control of the viscous Burgers equation using an equivalent index method. *Journal of Global Optimization*, 18:255–263, 2000.

[15] H. M. Park and Y. D. Jang. Control of Burgers equation by means of mode reduction. *International Journal of Engineering Science*, 38:785–805, 2002.

[16] W.-J. Liu and M. Krstić. Backstepping boundary control of Burgers equation with actuator dynamics. *Systems and Control Letters*, 41:291–303, 2000.

[17] W.-J. Liu and M. Krstić. Adaptive control of Burgers equation with unknown viscosity. *International Journal Adaptive Control and Signal Processing*, 15:745–766, 2001.

[18] M. Krstić. On global stabilization of Burgers equation by boundary control. *Systems and Control Letters*, 37:123–141, 1999.

[19] M. Ö. Efe and H. Özbay. Integral action based Dirichlét boundary control of Burgers equation. *Proceedings of the IEEE International Conference on Control Applications* (CCA'2003), Istanbul, Turkey, 23–25 June, pp. 1267–1272, 2003.

[20] M. Ö. Efe, X. Yuan, H. Özbay and M. Samimy. Interpolating local models of POD using fuzzy decision mechanisms. *9th Mechatronics Forum International Conference*, 30 August–1 September, Ankara, Turkey, pp. 347–356, 2004.

[21] M. Ö. Efe and H. Özbay. Low dimensional modeling and Dirichlét boundary controller design for Burgers equation. *International Journal of Control*, 77(10):895–906, 2004.

[22] S. S. Ravindran. A reduced order approach for optimal control of fluids using proper orthogonal decomposition. *International Journal for Numerical Methods in Fluids*, 34:425–488, 2000.

[23] S. N. Singh, J. H. Myatt, G. A. Addington, S. Banda and J. K. Hall. Optimal feedback control of vortex shedding using proper orthogonal decomposition models. *Transactions of the ASME: Journal of Fluids Engineering*, 123:612–618, 2001.

[24] H. V. Ly and H. T. Tran. Modeling and control of physical processes using proper orthogonal decomposition. *Mathematical and Computer Modelling of Dynamical Systems*, 33:223–236, 2001.

[25] J. Lumley. The structure of inhomogeneous turbulent flows. In: A. M. Yaglom and V. I. Tatarski (eds), *Atmospheric Turbulence and Wave Propagation*. Moscow: Nauka, pp. 166–176, 1967.

[26] M. Ö. Efe and H. Özbay. Proper orthogonal decomposition for reduced order modeling: 2D heat flow. *Proceedings of the IEEE International Conference on Control Applications* (CCA'2003), Istanbul, Turkey, 23–25 June, pp. 1273–1278, 2003.

[27] C. W. Rowley, T. Colonius and R. M. Murray. Model reduction for compressible flows using POD and Galerkin projection. *Physica D-Nonlinear Phenomena*, 189(1–2):115–129, 2004.

[28] C. W. Rowley. Model reduction for fluids, using balanced proper orthogonal decomposition. *International Journal of Bifurcation and Chaos*, 15(3):997–1013, 2005.

[29] S. Gügercin and A. C. Antoulas. A survey of model reduction by balanced truncation and some new results. *International Journal of Control*, 77(8):748–766, 2004.

[30] L. Sirovich. Turbulence and the dynamics of coherent structures. *Quarterly of Applied Mathematics*, XLV(3):561–590, 1987.

[31] K. Willcox and J. Peraire. Balanced model reduction via the proper orthogonal decomposition. *15th AIAA Computational Fluid Dynamics Conference*, 11–14 June, AIAA 2001–2611, 2001.

[32] S. J. Farlow. *Partial Differential Equations for Scientists and Engineers*. New York: Dover Publications Inc., pp. 317–322, 1993.

[33] L. Baramov, O. R. Tutty and E. Rogers. $\mathcal{H}_\infty$ control of non-periodic two dimensional channel flow. *IEEE Transactions on Control Systems Technology*, 12:111–122, 2002.

[34] L. Baramov, O. R. Tutty and E. Rogers. Robust control of linearized Poiseuille flow. *AIAA Journal of Guidance, Dynamics, and Control*, 25:145–151, 2002.

[35] G. Lassaux and K. Willcox. Model reduction for active control design using multiple-point Arnoldi methods. *41st Aerospace Sciences Meeting Exhibit*, Reno, NV, USA, AIAA 2003-0616, 2003.

[36] O. M. Aamo and M. Krstić. *Flow Control by Feedback*. London: Springer-Verlag, 2003.